

Assessment of the photosynthetically active incident radiation in outdoor photobioreactors using oxalic acid/uranyl sulfate chemical actinometer

A. Sánchez Mirón, E. Molina Grima, J.M. Fernández Sevilla, Y. Chisti & F. García Camacho*
Department of Chemical Engineering, University of Almería, E-04071 Almería, Spain

(*Author for correspondence; fax +34-950-21-5484; e-mail fgarcia@ualm.es)

Received 1 October 1999; revised 4 March 2000; accepted 11 April 2000

Key words: actinometry, incident photon flux, photobioreactor

Abstract

A simple actinometric method was evaluated for measuring the photosynthetically active incident photon flux on outdoor photobioreactors. The method is based on uranyl sulfate catalyzed photodecomposition of oxalic acid in presence of light. The uranyl–oxalate chemical actinometer absorbs radiation of wavelengths below 535 nm. In the present work, the photobioreactor wall material did not transmit light energy of wavelengths below 350 nm and the effective absorptivity method was used to evaluate the photon flux between 350–535 nm. The standard solar spectrum of the American Society for Testing and Materials (ASTM) was employed for estimating the ratio between the photosynthetically active radiation (400–700 nm) and the solar radiation in the 350–535 nm range. This ratio (2.21) was taken to be equal to the quotient between the photosynthetically active radiation (PAR) and the incident photon flux on the photobioreactor's surface (for the solar radiation between 350–535 nm). PAR measurements with 4π spherical and 2π quantum sensors were used to validate the method.

Nomenclature

ASTM	American Society for Testing and Materials
C_A	Cell concentration, kg m^{-3}
C_{ox}	Concentration of oxalic acid, M or kg m^{-3}
E_λ	Solar irradiance energy at wavelength λ , $\text{W m}^{-2}\text{nm}^{-1}$
F_{abs}	Quantity of radiation absorbed, $\mu\text{mol photon m}^{-3}\text{s}^{-1}$
F_o	Incident light flux, $\mu\text{mol photon m}^{-3}\text{s}^{-1}$
$(F_o)_{350\text{nm}}^{535\text{nm}}$	Incident photon flux in the wavelength range of 350–535 nm, $\mu\text{mol photon m}^{-3}\text{s}^{-1}$
F_{vol}	Photon flux absorbed in reactor volume, $\mu\text{mol photon m}^{-3}\text{s}^{-1}$
$(F_{vol})_{max}$	Maximum absorbed photon flux, $\mu\text{mol photon m}^{-3}\text{s}^{-1}$
F_1	Factor in Eqn (2), dimensionless
f'_λ	Ratio defined by Eqn (6), dimensionless
I_{av}	Average irradiance inside the culture, $\mu\text{mol photon m}^{-2}\text{s}^{-1}$
I_o	Irradiance measured (4π sensor) at the center of the photobioreactor, $\mu\text{mol photon m}^{-2}\text{s}^{-1}$
K_a	Light absorption coefficient of the biomass, $\text{m}^2 \text{kg}^{-1}$
L	Depth of channel, m
PAR	Photosynthetically active radiation

P_D	Photosynthetic photon flux density or the quantum flux density, $\mu\text{mol photon m}^{-2} \text{s}^{-1}$
P_F	Photosynthetic photon flux fluence rate, $\mu\text{mol photon m}^{-2} \text{s}^{-1}$
PVC	Poly(vinyl chloride)
R	Radius of the reactor, m
R_{ox}	Rate of photooxidation, $\text{kmol m}^{-3} \text{s}^{-1}$
T_λ	Transmittance of poly(methyl methacrylate) at wavelength λ , dimensionless
UV	Ultraviolet radiation

Greek symbols:

β	Parameter in Eqn (3), $\text{m}^3 \text{kg}^{-1}$ or $\text{m}^3 \text{kmol}^{-1}$
μ	Mean molar absorption coefficient or absorptivity, $\text{m}^2 \text{kmol}^{-1}$
μ_λ	Absorption coefficient at wavelength λ , $\text{m}^2 \text{kg}^{-1}$ or $\text{m}^2 \text{kmol}^{-1}$
λ	Wavelength, nm
π	Pi
Φ_p	Average primary quantum yield for the actinometer absorption range, $\text{kmol (kmol photon)}^{-1}$
Φ_λ	Quantum yield of photodecomposition at wavelength λ , $\text{kmol (kmol photon)}^{-1}$

Introduction

Outdoor photobioreactors are commonly used for large-scale culture of microalgae. Quantification of photosynthetically active radiation (PAR, 400–700 nm wavelength) is needed for photobioreactor engineering, to establish the microalgal growth efficiency and the quantum yield (Aiba, 1982; Lee et al., 1984; Molina Grima et al., 1997).

Among the main factors influencing the determination of quantum yield is the difficulty of modeling the solar photon flux incident on the surface of a photobioreactor. Some of the causes of this difficulty are: 1. Variation in solar radiation levels with the time of day and season; 2. the fact that the incident radiation is made up of a direct and a diffuse component with mutually varying proportions; 3. contribution of reflected radiation from the surroundings; and 4. a non-homogeneous distribution of the direct solar radiation on curved surfaces of photobioreactors or on photobioreactors with unusual geometries such as the helical biocoil photobioreactor (Watanabe et al., 1995), the α -reactor (Lee et al., 1995).

An imprecise determination of the incident photon flux affects the accuracy of the calculated quantum yield and the evaluation of photobioreactors. Modeling of photobioreactors attempts to relate the light available to the growth kinetics of the alga (Cornet et al., 1995; Ación Fernández et al., 1997; García Camacho et al., 1999). Thus, the light distribution inside a photobioreactor needs to be accurately modeled and,

hence, the incident photon flux needs to be known reasonably well.

The total photosynthetically active photon flux incident on a reactor may be determined by one of three methods:

1. In a vertical reactor of cylindrical geometry, illuminated radially with a homogeneous incident light flux, F_o , on one side of the reactor, the flux F_o can be measured as the photosynthetic photon flux fluence rate (P_F), also referred to as the quantum scalar irradiance or the photospherical irradiance. This is the integral photon flux at a point from all directions around the point. In a cylindrical reactor illuminated with perfectly diffuse light, the relation between P_F and F_o , for pure water in the reactor, is (Contreras et al., 1998):

$$F_o = \frac{2P_F}{\pi R} \quad (1)$$

2. Using a cosine (180°) quantum sensor which provides the photosynthetic photon flux density (P_D), also referred to as the quantum flux density. Photosynthetic photon flux density is the number of photon in the 400–700 nm (PAR) waveband incident on a unit surface per unit time. A cosine sensor is ideal for measurements on flat surfaces, but it may be used also for point measurements on a curved surface. For the latter case, measurements from several points would need to be averaged to obtain the flux entering the reactor.

- Using a chemical actinometer. This procedure is especially indicated in those cases where the other two methods are unsatisfactory, for example, when the bioreactor geometry is of an unusual type, when the radiation arrives from multiple directions (e.g., diffuse radiation), or when a theoretical radiation field inside a photobioreactor needs to be checked.

In chemical actinometry, the incident light flux F_0 is obtained from the measured rate of a photochemical reaction for which the quantum yield is well-known (Cornet et al., 1997). Only a few photochemical reactions with well-known and constant quantum yields have been documented for use in the range of wavelengths that are of interest in photosynthesis (400–700 nm). One such actinometer is the Reinecke's salt, as described by Wegner & Adamson (1966). Reinecke's salt actinometer has a constant quantum yield in the light wavelength range of 316–750 nm, but two constraints are associated with its use: (i) the solution needs to be prepared outside the photobioreactor; and (ii) the actinometer is extremely sensitive to light and, hence, its use in pilot scale operations is inconvenient.

Other known actinometers for the visible spectral range also pose problems. For example, photooxidation of chromium urea salt and thiourea (Warburg & Schocken, 1949; Wegner & Adamson, 1966) are only suitable for narrow ranges of wavelengths and some of these organic compounds affect materials such as poly(vinyl chloride) and methacrylate polymers that are used in construction of the photobioreactors.

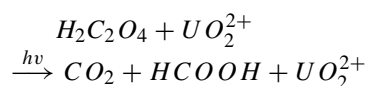
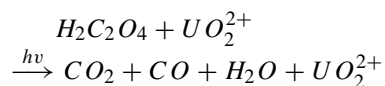
Consequently, the selection of rapid and satisfactory actinometers to determine the absorbed photon flux in the visible range of solar spectrum is not easy. A compilation of photochemical systems suitable for integrating the incident light by chemical conversion is given by Kuhn et al. (1989). One actinometer that stands out in the list, is the uranyl sulfate catalyzed photooxidation of oxalic acid. The use of this system is well-established (Martín et al., 1996a; Rosseti et al., 1998) and its other outstanding characteristics are: a clearly established dependence between quantum yield and the wavelength for the wavelength range of interest; relative insensitivity of quantum yield to changes in temperature; well-defined zero-order kinetics of the reaction with respect to oxalic acid concentration; a quantum yield that is independent of the irradiance level; an absence of dark reactions; and ease of use for pilot scale measurements (Curcó et al., 1996).

So far, the uranyl oxalate actinometer has been used mainly to quantify the incident UV radiation in reactors for photocatalytic destruction of water pollutants. This work demonstrates the use of uranyl sulfate/oxalic acid system for quantifying the photosynthetically active photon flux incident on outdoor photobioreactors. The method is validated by parallel measurements of incident radiation flux using a spherical quantum sensor and a cosine (180°) quantum sensor.

Materials and methods

Actinometry

Photodecomposition of oxalic acid in presence of uranyl sulfate catalyst was the actinometric system used. The reaction was initiated by mixing aqueous solutions of oxalic acid and uranyl sulfate in 5:1 molar ratio. The overall photochemical reaction may be written as (Rosseti et al., 1998):



To avoid parallel reactions such as the reduction of uranyl sulfate, it is necessary to maintain the conversion below 20%. Within the noted conversion limit, the overall reaction is zero-order with respect to the concentration of oxalic acid. The uranyl sulfate catalyst is of course not consumed during the reaction. Also, as the concentration of uranyl sulfate is constant during actinometry, the light absorption coefficient does not change with time. Within the noted conversion limit, any parallel reactions and/or dark reactions are minimal (Leighton & Forbes, 1930).

Setup

The schematic experimental setup is illustrated in Figure 1. Two identical transparent 5-L (working volume) vessels were used in the measurements. Both vessels were 0.096 m in diameter and 0.69 m in height. The vessels were made of poly(methyl methacrylate), a material that is commonly used in construction of photobioreactors (García Camacho et al., 1998; Sánchez Mirón et al., 1999). One of the tubes was used for the photoreaction; the second tube, filled with distilled water, was used to measure the incident photon flux

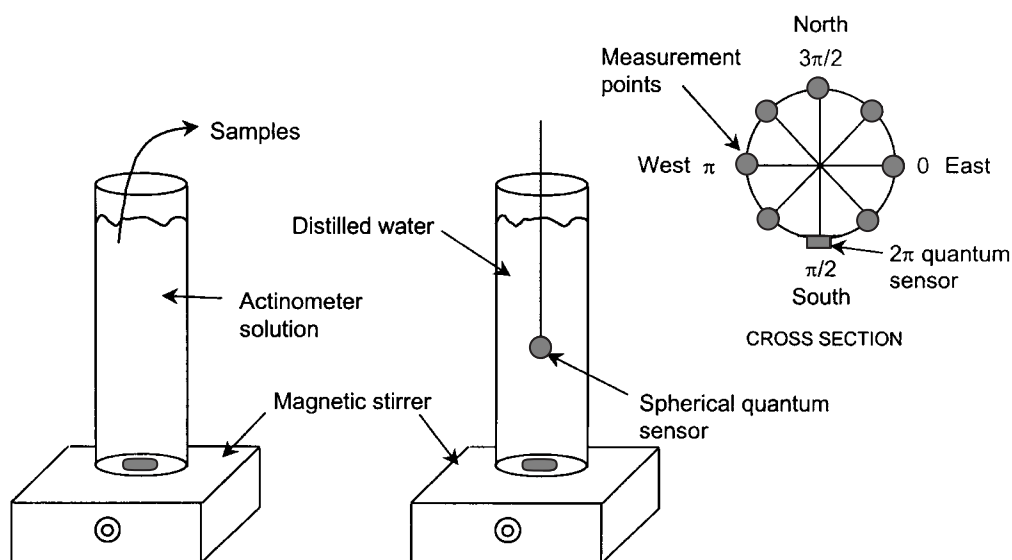


Figure 1. Schematic of the measurement system.

density P_F at the center of the tube and the P_D values at several points on the surface. The measurements at the center of the photoreactor used a quantum scalar irradiance sensor (QSL-100, Biospherical Instruments, San Diego, CA). The measurements at the surface used a 2π sensor (LI-190SA, Li-cor, Inc., Lincoln, NE).

The transmissivity spectrum of poly(methyl methacrylate) is shown in Figure 2 along with spectra of other materials commonly used to manufacture photobioreactors. Unlike glass, the methacrylate and PVC plastics transmit little ultraviolet light. This aspect is important because certain species of algae are inhibited by UV radiation. For example, photosynthesis in the diatoms *Phaeodactylum tricornutum* Bohlin (NEPCC clone 31) and *Thalassiosira pseudonna* is inhibited by UV radiation in a manner that depends on radiation dose and dosage rate (Cullen & Lesser, 1991; Behrenfeld et al., 1992).

Procedure

For the measurements, 5 L of actinometric solution was prepared in the photobioreactor, and the magnetic stirrer was turned on. During this period, the reactor was covered with opaque paper to prevent entry of solar radiation. After a few minutes of mixing, a 5-mL sample was withdrawn from the reactor as the zero time sample and the opaque paper cover was removed. Samples were taken at equal time intervals until the experimental run was complete. The total run time was

25 to 30 min. Oxalic acid concentration of each sample was measured by conventional titration with 0.1 N potassium permanganate. Within a single experimental run, the liquid volume in the reactor did not change by more than 1% of the initial value. This change in volume had no significant effect on the results, as confirmed experimentally.

Principles and the problem

As in any photocatalytic process, the rate of photosynthesis depends on the quantity of radiation absorbed (F_{abs}) by the cells. To estimate F_{abs} , we need to know how much of the incident photon flux on a reactor's surface enters the vessel. Thus, the radiation absorbed by the catalyst is related to the incident radiation by a factor, F_1 (Curcó, 1996):

$$F_{abs} = F_o \cdot F_1. \quad (2)$$

The value of the factor F_1 may be calculated in three ways: (i) using published theoretical models (Cornet et al., 1995); (ii) turbidimetric models (Yokota et al., 1989); and (iii) using the effective absorptivity method (Curcó, 1996).

The effective absorptivity method is based on the use of a function of Lambert-Beer law type, and, for an absorbing medium, leads to:

$$F_{abs} = F_o[1 - \exp(-\beta C_A)]. \quad (3)$$

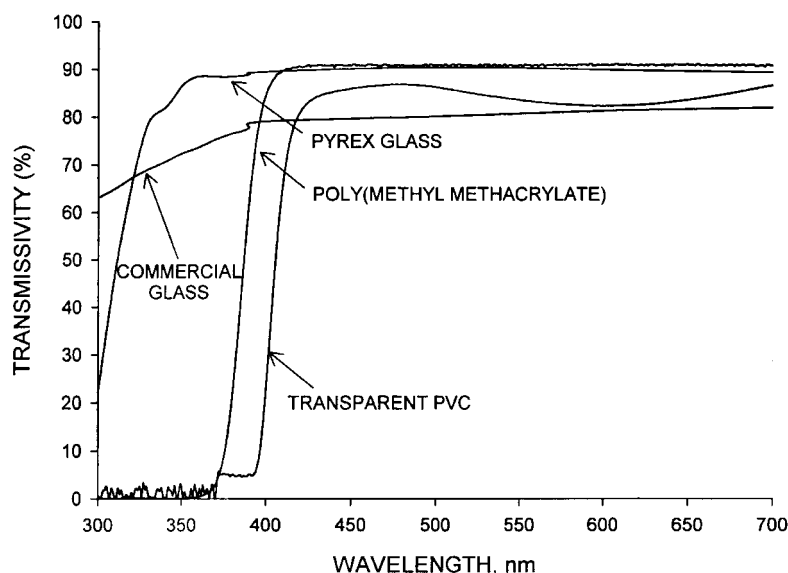


Figure 2. Light absorption spectra of some materials used in photobioreactor construction.

The value of the parameter β depends on light distribution on the surface of a photobioreactor (Cornet et al., 1997). For a rectangular reactor illuminated on one side, $\beta = \mu \cdot L$, where L is the depth of the channel. Similarly, for a cylindrical reactor illuminated radially, $\beta = 2\mu \cdot R$ where R is the radius of the reactor. The incident flux F_0 is assumed to be homogeneous on the rear surface of the reactor, μ is the mean molar absorption coefficient or absorptivity, and C_A is the particle or cell concentration. The product $\mu \cdot C_A$ is the mean absorptivity coefficient of the suspension.

Under similar or identical experimental conditions (radiation source, spectral distribution, species, biomass concentration, reactor geometry, etc.), the factor F_1 is independent of scale. So, if F_1 is known and F_0 cannot be measured directly by sensors (e.g., in reactors of complex geometries), actinometric measurements using photochemical reactions become necessary. In these reactions, the rate depends on the intensity and spectral distribution characteristics of the incident light. The spectral data for the absorption coefficient (μ_λ) of the uranyl oxalate solution and the quantum yield (Φ_λ) of the uranyl oxalate photodecomposition are shown in Figure 3 for a wavelength range of 300 to 535 nm, according to Cassano et al. (1968) and Martín et al. (1996a).

As the variables μ_λ and Φ_λ are wavelength dependent, and the radiation source is not monochromatic, the decomposition rate is written as follows:

$$-\frac{dC_{ox}}{dt} = R_{ox} = \Phi_p \sum_{\lambda=350nm}^{535nm} F_{abs,\lambda} \quad (4)$$

where C_{ox} is the oxalic acid concentration and Φ_p is the average primary quantum yield over the radiation absorption range of the actinometer (Martín et al., 1996b):

$$\Phi_p = \frac{\sum_{\lambda=350nm}^{535nm} E_\lambda \Phi_\lambda}{\sum_{\lambda=350nm}^{535nm} E_\lambda} \quad (5)$$

In Eqn (5), E_λ is the solar irradiance at wavelength λ . Although, the wavelength range of the actinometer is between 200 and 535 nm, the sumatory limits in Eqn (4) and Eqn (5) are 350 to 535 nm because the reactor wall material (poly(methyl methacrylate)) filters out the solar radiation of wavelengths less than 350 nm.

Measurements of spectral solar irradiance, provided by the Plataforma Solar de Almería, Spain, were used for characterizing the light source. As expected, E_λ , varied with the time of year and also with the time of day. However, the normalized spectra, obtained by dividing E_λ at each wavelength by the integrated irradiance in the considered wavelength range were similar for different days. As these normalized spectra matched (Figure 4) with the standard spectrum of the ASTM, the ASTM spectrum was used for all work reported.

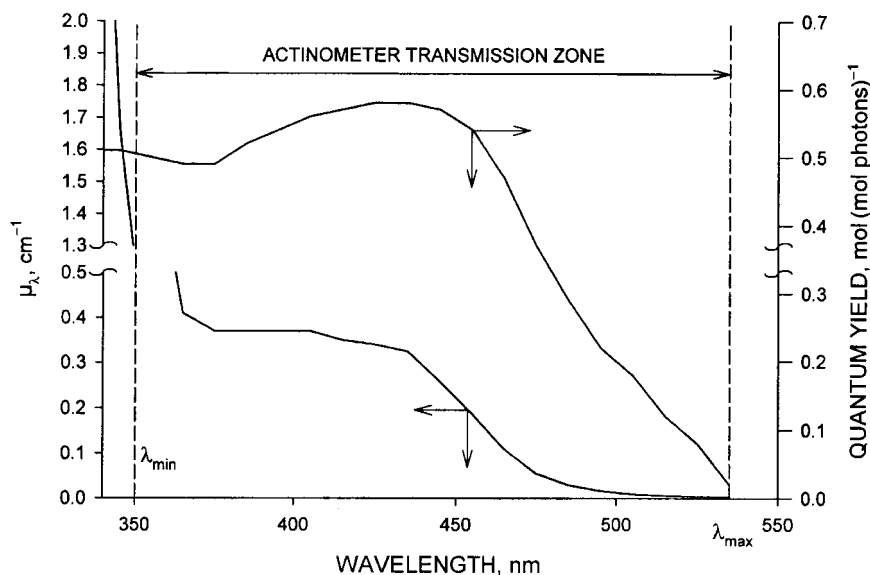


Figure 3. Absorption coefficient of the reactant solution (μ_λ) and the quantum yield of the photodecomposition as a function of wavelength. The light transmission range for the actinometer is also shown.

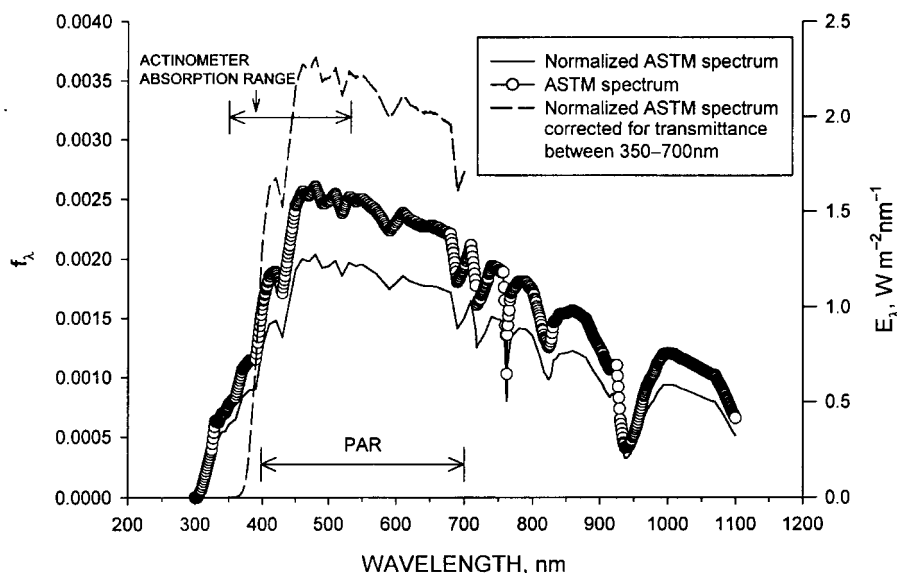


Figure 4. Comparison of the various normalized spectra with the ASTM standard spectrum.

Because the poly(methyl methacrylate) reactor wall material transmits only above a wavelength of 350 nm and the wavelength range of interest is the visible portion of the solar spectrum, the ASTM data (Figure 4) was normalized between 350 and 700 nm. The equation used for normalizing was as follows:

$$f'_\lambda = \frac{E_\lambda T_\lambda}{\sum_{\lambda=350\text{nm}}^{700\text{nm}} E_\lambda T_\lambda} \quad (6)$$

where T_λ is the transmittance of poly(methyl methacrylate) at the wavelength λ (Figure 2).

In consequence, using the normalized spectral data of Figure 4, the photosynthetically active incident photon flux (400–700 nm), i.e. $(F_o)_{400\text{nm}}^{700\text{nm}}$, can be calculated as a function of the incident photon flux in the wavelength range of 350–535 nm, i.e. $(F_o)_{350\text{nm}}^{535\text{nm}}$ or vice versa. The 350–535 nm range is where the actinometer absorbs. Thus,

$$\frac{\sum_{\lambda=400\text{nm}}^{700\text{nm}} E_{\lambda}}{\sum_{\lambda=350\text{nm}}^{535\text{nm}} E_{\lambda}} = \frac{\sum_{\lambda=400\text{nm}}^{700\text{nm}} f'_{\lambda}}{\sum_{\lambda=350\text{nm}}^{535\text{nm}} f'_{\lambda}} = 2.21 = \frac{(F_o)_{400\text{nm}}^{700\text{nm}}}{(F_o)_{350\text{nm}}^{535\text{nm}}} \quad (7)$$

Where $(F_o)_{350\text{nm}}^{535\text{nm}}$ is obtained using $(F_{\text{abs}})_{350\text{nm}}^{535\text{nm}}$ (i.e. the measured photon flux absorption of the actinometer) and Eqn (3); thus,

$$\left[(F_o)_{350}^{535} \right]_{\lambda} = (F_o)_{350}^{535} f'_{\lambda} = \frac{[(F_{\text{abs}})_{350}^{535}]_{\lambda}}{1 - \exp(-2\mu_{\lambda}R)} \quad (8)$$

and

$$(F_o)_{350}^{535} = \frac{\sum_{\lambda=350\text{nm}}^{535\text{nm}} [(F_{\text{abs}})_{350}^{535}]_{\lambda}}{\sum_{\lambda=350\text{nm}}^{535\text{nm}} f'_{\lambda} [1 - \exp(-2\mu_{\lambda}R)]} \quad (9)$$

where

$$\sum_{\lambda=350\text{nm}}^{525\text{nm}} [(F_{\text{abs}})_{350}^{535}]_{\lambda} = (F_{\text{abs}})_{350}^{535} \quad (10)$$

Results and discussion

Incident photon flux, F_o , from the 2π quantum sensor

A measured incident photon flux density (P_D) profile is shown in Figure 5. The profile was obtained using the 2π irradiance sensor at solar noon. As expected, the values measured along the circumference facing the Sun show a parabolic variation with position. The incident photon flux on the side opposite to the Sun was roughly constant irrespective of position. The latter, constant P_D value corresponded to illumination by diffuse radiation. So, the P_D values measured along the circumference facing the Sun could be divided into a contribution from direct radiation and one from diffused radiation. The latter was equivalent to the mean P_D value obtained on the side opposite to the Sun. According to LICOR catalog, there is no unique relationship between P_D and P_F . For a collimated beam (direct radiation) at normal incidence, P_D and P_F are equal; while for perfectly diffuse radiation, the P_F is 4 times the P_D . Thus, the mean total P_D was corrected by multiplying the diffuse P_D value by 4, as recommended by LICOR, the manufacturer of the 2π sensor. The

incident photon flux, $(F_o)_{400\text{nm}}^{700\text{nm}}$, was estimated by multiplying the mean P_D by the surface-to-volume ratio of the photobioreactor.

Incident photon flux, F_o , from the 4π spherical quantum sensor

As mentioned earlier, the photon fluence rate P_F is the integral of the photon flux incident at a point from all directions around the point. As a result, the response of a 4π sensor to a certain irradiance level is the same, irrespective of whether the radiation is direct, diffuse, reflected, and so forth. From light field modeling in microalgal cultures grown in cylindrical vessels and illuminated with diffuse light, Molina Grima et al. (1997) obtained the following equation for photon flux absorbed (F_{vol}) in the reactor volume:

$$F_{\text{vol}} = I_{\text{av}} K_a C_A \quad (11)$$

where K_a is the light absorption coefficient for the biomass, C_A is the biomass concentration, and I_{av} is the average irradiance inside the culture. The I_{av} is given by the equation (Molina Grima et al., 1997):

$$I_{\text{av}} = \frac{2 \cdot I_o}{R \cdot K_a \cdot C_A} \quad (12)$$

$$\left(1 - \int_0^{\pi/2} \cos(\phi) \cdot \exp[-2 \cdot R \cdot K_a \cdot C_A \cdot \cos(\phi)] \cdot d\phi \right)$$

In Eqn (12), I_o is the irradiance measured at the center of the photobioreactor with the 4π sensor, and R is the radius of the reactor. If the culture extinction $K_a \cdot C_A$ is infinite, all incident photon flux is absorbed and $(F_o)_{400\text{nm}}^{700\text{nm}}$ equals the maximum absorbed photon flux $(F_{\text{vol}})_{\text{max}}$. The $(F_{\text{vol}})_{\text{max}}$ value was obtained from the limit of Eqn (11) when $K_a \cdot C_A$ tends to infinity (Contreras et al., 1998):

$$(F_{\text{vol}})_{\text{max}} = (F_o)_{400\text{nm}}^{700\text{nm}} = \frac{2 P_F}{\pi R} \quad (13)$$

Figure 6 compares the $(F_o)_{400\text{nm}}^{700\text{nm}}$ values obtained from both the P_D and P_F measurements for a given day. As shown in the figure, about 90% of the F_o data matched within $\pm 15\%$, irrespective of how they were obtained. Consequently, both measurement methods may be considered equivalent for determining $(F_o)_{400\text{nm}}^{700\text{nm}}$ values. Because manual logging of P_D data is laborious, on-line acquired P_F data were used to calculate $(F_o)_{400\text{nm}}^{700\text{nm}}$ in all subsequent measurements.

Photon flux from chemical actinometry

The photobioreactor used earlier for measurements with 2π and 4π sensors, was later used in chemical

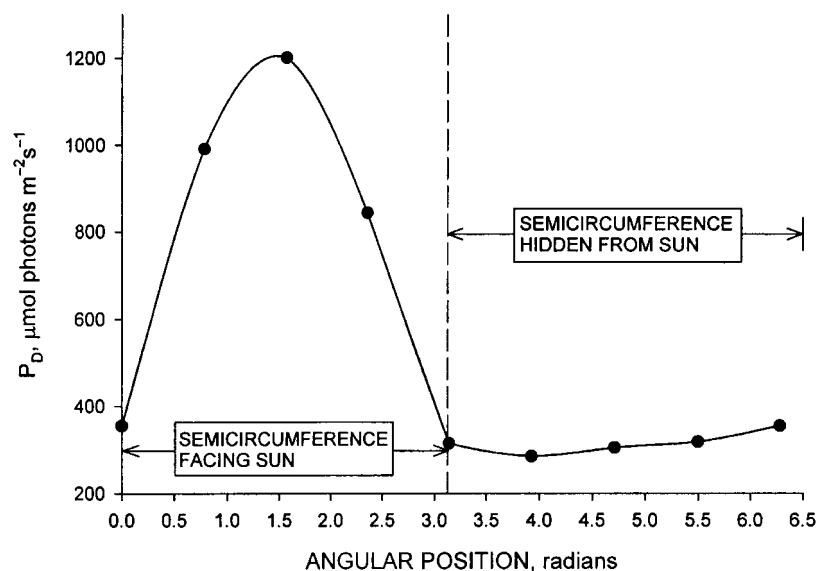


Figure 5. The midday profile of photosynthetic photon flux density around the circumference of the tubular photoreactor vessel.

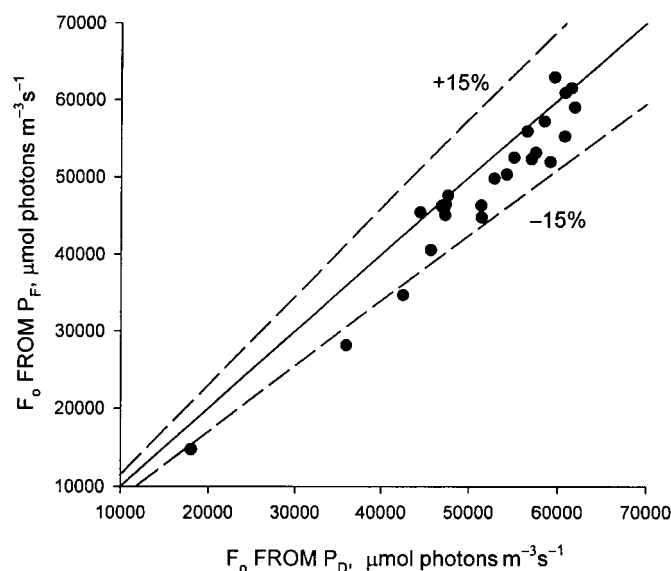


Figure 6. Comparison of the F_o values obtained by measurements of photosynthetic photon flux density (P_D) and the photosynthetic photon fluence rate (P_F). The solid line represents an exact match.

actinometric measurements. The time course of photodecomposition of aqueous oxalic acid solutions is shown in Figure 7. The figure illustrates two runs carried out at different incident photon flux values, as determined by a spherical quantum sensor. The data are presented as concentration of oxalic acid. The decline in concentration is linear (Figure 7), as expected of zero-order kinetics and a constant decomposition rate during the period of interest. The $(F_{\text{abs}})_{350\text{nm}}^{535\text{nm}}$

value was calculated using the measured rate data in Eqn (4). The $(F_o)_{400\text{nm}}^{700\text{nm}}$ values were estimated using suitably modified Eqn (9).

All the $(F_o)_{400\text{nm}}^{700\text{nm}}$ values obtained from the measurements of P_F and from the actinometric method are compared in Figure 8. The two methods agree to within $\pm 15\%$ deviation for nearly all the data. This, and data in Figure 6 confirm that all three methods (the chemical actinometer, 2π and 4π sensors) for

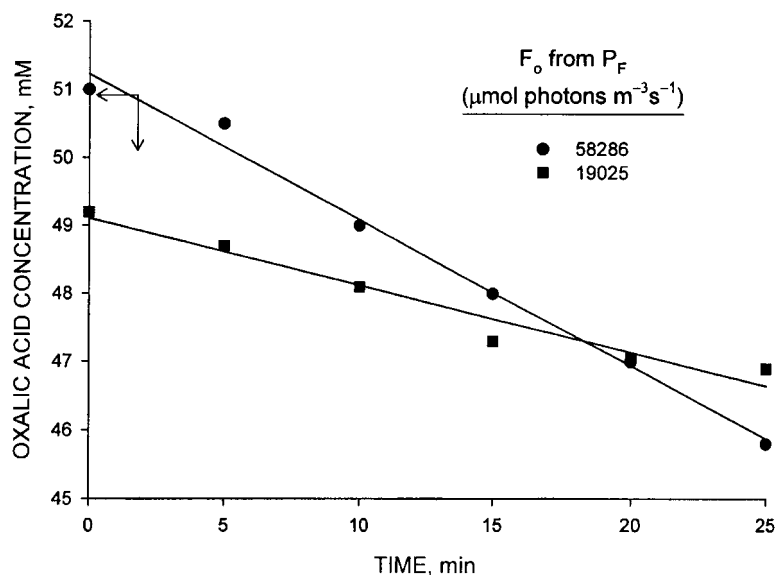


Figure 7. Photodecomposition of oxalic acid at different incident photon flux (F_0) values. Data are shown for concentration and conversion versus time.

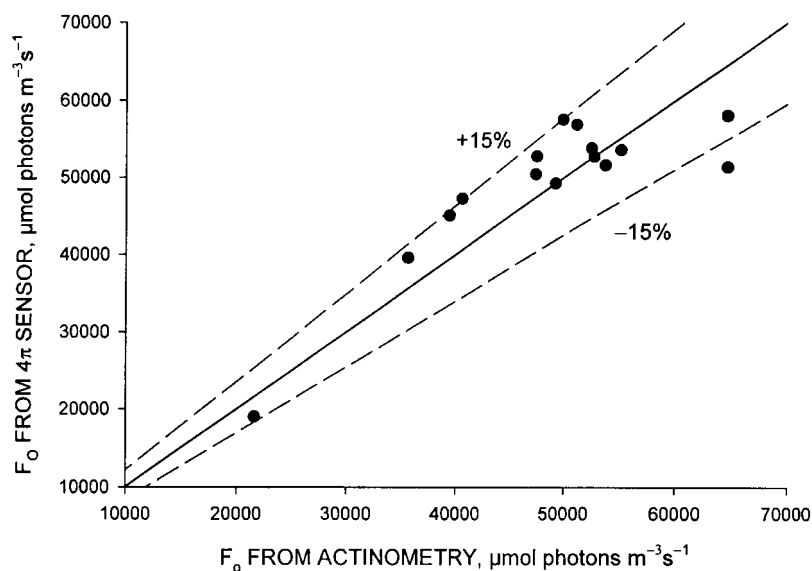


Figure 8. Comparison of the incident solar radiation flux data obtained with chemical actinometry and 4π sensor. The solid line represents an exact match.

evaluating the mean photosynthetically active photon flux, $(F_0)_{400\text{nm}}^{700\text{nm}}$, in a photobioreactor are consistent when used correctly. Thus, the uranyl oxalate actinometric method may be used as a reference measurement in photobioreactors where complexities of geometry do not permit a satisfactory implementation of sensor-based measurement methods. The uranyl oxalate photodecomposition can be satisfactorily used

with a polychromatic light source such as sunlight. The existing standard methods relying on 4π spherical quantum sensors at the center of a reactor and 2π quantum sensors on reactor's surface are easy to use, but they are satisfactory only for photobioreactors with rectangular, cylindrical, or other simple geometry.

In comparison with the Reinecke's salt actinometer the uranyl oxalate actinometer is rapid and better

suiting to outdoor measurements where the irradiance level changes with time. For example, the total measurement duration in this work was only 25 min versus 2 h for measurements using Reinecke's salt (Cornet et al., 1997).

In outdoor conditions, over a 2-h interval, the illumination level can change greatly: for example, between 0900 and 1100, the increment in irradiance may be as much as $1100 \mu\text{mol photon m}^{-2}\text{s}^{-1}$. Over a 25-min period, the increment would be about $229 \mu\text{mol photon m}^{-2}\text{s}^{-1}$, or a mere 20% of the value over the longer period. Over a 25 min period, the solar irradiance level may be assumed constant without significantly affecting the calculated estimate $(F_0)_{400\text{nm}}^{700\text{nm}}$.

Conclusions

Chemical actinometry using uranyl sulfate catalyzed photodecomposition of oxalic acid as the measuring reaction, can be effectively employed for establishing the photosynthetic light flux in photobioreactors especially ones with complicated geometries. When correctly used, actinometric measurements are consistent with those from 2π and 4π quantum sensors. The only real limitation of the method is the toxicity of the uranyl salts. Toxicity limits the maximum volume that may be handled easily and disposed of subsequent to use.

Acknowledgements

This research was supported by the Comision Interministerial de Ciencia y Tecnologia (CICYT) (BIO98-0522), Spain. We thank Dr Sixto Malato Rodríguez, Plataforma Solar de Almería, Spain, for helpful advice. Cristobal Sánchez Martín is thanked for technical assistance.

References

Acién Fernández FG, García Camacho F, Sánchez Pérez JA, Fernández Sevilla JM, Molina Grima E (1997) A model for light distribution and average solar irradiance inside outdoor tubular photobioreactors for the microalgal mass culture. *Biotechnol. Bioengng* 55: 701–714.

Aiba S (1982) Growth kinetics of photosynthetic microorganisms. *Adv. Biochem. Engng* 23: 85–156.

Behrenfeld MJ, Hardy JT, Lee H (1992) Chronic effects of ultraviolet-B radiation on growth and cell volume of *Phaeodactylum tricornutum* (Bacillariophyceae). *J. Phycol.* 28: 757–760.

Cassano AE (1968) Uso de actinómetros en reactores tubulares continuos. *Revista de la Facultad de Ingeniería Química* 37: 469–501.

Contreras A, García F, Molina E, Merchuk JC (1998) Interaction between CO₂-mass transfer, light availability, and hydrodynamic stress in the growth of *Phaeodactylum tricornutum* in a concentric tube airlift photobioreactor. *Biotechnol. Bioeng.* 60: 317–325.

Cornet JF, Dussap CG, Gross JB, Binois C, Lasseur C (1995) A simplified monodimensional approach for modelling coupling between radiant light transfer and growth kinetics in photobioreactors. *Chem. Eng. Sci.* 50: 1489–1500.

Cornet JF, Marty A, Gros JB (1997) Revised technique for the determination of mean incident light fluxes on photobioreactors. *Biotechnol. Progr.* 13: 408–415.

Cullen JJ, Lesser MP (1991) Inhibition of photosynthesis by ultraviolet radiation as a function of dose and dosage rate: results for a marine diatom. *Mar. Biol.* 111: 183–190.

Curcú D, Malato S, Blanco J, Giménez J (1996) Photocatalysis and radiation absorption in a solar plant. *Solar Energy Materials and Solar Cells* 44: 199–217.

García Camacho F, Contreras Gómez A, Acién Fernández FG, Fernández Sevilla J, Molina Grima E (1999) Use of concentric-tube airlift photobioreactors for microalgal outdoor mass cultures. *Enzyme Microb. Technol.* 24: 164–172.

Kuhn HJ, Braslavsky SE, Schmidt R (1989) Chemical actinometry. *Pure appl. Chem.* 61(2): 187–210.

Lee HY, Erickson LE, Yang SS (1984) The estimation of growth yield and maintenance parameters for photoautotrophic growth. *Biotechnol. Bioengng* 26: 926–935.

Lee YK, Ding SY, Low, CS, Chang YC, Forday, WL, Chew PC (1995) Design and performance of an alpha-type tubular photobioreactor for mass cultivation of microalgae. *J. appl. Phycol.* 7: 47–51.

Leighton WG, Forbes GA (1930) Precision actinometry with uranyl oxalate. *J. Am. Chem. Soc.* 52: 3139–3152.

Martín CA, Baltanás MA, Cassano, AE (1996a) Photocatalytic reactors. II. Quantum efficiencies allowing for scattering effects. An experimental approximation. *J. Photochem. Photobiol. A: Chem.* 94: 173–189.

Martín CA, Baltanás MA, Cassano AE (1996b) Photocatalytic reactors. 3. kinetics of the decomposition of chloroform including absorbed radiation effects. *Environ. Sci. Technol.* 30: 2355–2364.

Molina Grima E, García Camacho F, Sánchez Pérez JA, Acién Fernández FG, Fernández Sevilla JM (1997) Evaluation of photosynthetic efficiency in microalgal cultures using averaged irradiance. *Enzyme Microb. Technol.* 21: 375–381.

Rossetti GH, Albizzati ED, Alfano, OM (1998) Modeling and experimental verification of a flat-plate solar photoreactor. *Ind. Eng. Chem. Res.* 37: 3592–3601.

Sánchez Mirón AS, Gómez Contreras A, García Camacho FG, Molina Grima E, Chisti Y (1999) Comparative evaluation of compact photobioreactors for large-scale monoculture of microalgae. *J. Biotechnol.* 70: 249–270.

Warburg O, Schocken V (1949) A manometric actinometer for the visible spectrum. *Arch. Biochem.* 21: 363–369.

Watanabe Y, de la Noüe J, Hall DO (1995) Photosynthetic performance of a helical tubular photobioreactor incorporating the cyanobacterium *Spirulina platensis*. *Biotechnol Bioengng* 47: 261–269.

Wegner EE, Adamson, AW (1966) Photochemistry of complexes. III. Absolute quantum yields for the photolysis of some aqueous chromium (III) complexes. Chemical actinometry in the long wavelength visible region. *J. Am. Chem. Soc.* 88: 394–404.

Yokota T, Takahata Y, Nanjo H, Takahashi K (1989) Estimation of light intensity in a solid-liquid photoreaction system. *J. chem. Eng. Japan* 22: 537–542.